

Cannabidiol-Decorated Berberine-Loaded Microemulsions Improve IBS-D Therapy Through Ketogenic Diet-Induced Cannabidiol Receptors Overexpression

Xinyu Fan^{1,2,*}, Jiachen Shi^{1,*}, Ye Liu³, Mengqiu Zhang¹, Min Lu^{1,2}, Ding Qu^{1,2}

¹Affiliated Hospital of Integrated Traditional Chinese and Western Medicine, Nanjing University of Chinese Medicine, Nanjing, People's Republic of China; ²Jiangsu Province Academy of Traditional Chinese Medicine, Nanjing, People's Republic of China; ³The Second Affiliated Hospital of Nanjing University of Chinese Medicine, Nanjing University of Chinese Medicine, Nanjing, People's Republic of China

*These authors contributed equally to this work

Correspondence: Min Lu, Jiangsu Province Academy of Traditional Chinese Medicine, 100 Shizi Street, Hongshan Road Nanjing 210028, People's Republic of China, Email lmxlsr6666@163.com; Ding Qu, Jiangsu Province Academy of Traditional Chinese Medicine, 100 Shizi Street, Hongshan Road, Nanjing, 210028, People's Republic of China, Email quding1985@hotmail.com

Background: Berberine (BR) shows promise as a candidate for treating irritable bowel syndrome with diarrhea (IBS-D). However, the undesired physicochemical properties and poor oral absorption limit its clinical translation. A ketogenic diet (KD) can induce intestinal overexpression of cannabidiol (CB) receptors, which may offer a potential target for IBS-D-specific delivery of BR.

Methods: The microemulsions loaded with BR and decorated with cannabidiol (CBD/BR-MEs) were developed through a one-step emulsion method. The pharmaceutical behaviors of the CBD/BR-MEs were measured using dynamic light scattering and high-performance liquid chromatography. The efficacy of the anti-IBS-D therapy was evaluated by assessing fecal water content, Bristol score, and AWR score. The intestinal permeability were assessed through immunofluorescent staining of CB1 and ZO-1, respectively. The signaling of CREB/BDNF/c-Fos was also studied along with immunofluorescent and immunohistochemical examination of brain sections.

Results: The CBD/BR-MEs, which had a particle size of approximately 30 nm and a surface density of 2% (wt%) CBD, achieved greater than 80% (wt%) encapsulation efficiency of BR. The pharmacokinetics performance of CBD/BR-MEs was significantly improved in the KD-fed IBS-D rats than the standard diet-fed ones, which is highly related to intestinal expression of CB1 receptors. The treatment with CBD/BR-MEs and KD exhibited evident comprehensive advantages over the other groups in terms of anti-IBS-D efficacy. CBD/BR-MEs and KD synergistically decreased intestinal permeability. Moreover, the treatment with CBD/BR-MEs and KD not only blocked the CREB/BDNF/c-Fos signaling in the brain but also decreased the levels of neurotrophic factors, neurotransmitters, and inflammatory cytokines in the serum of IBS-D model rats.

Conclusion: Such a design represents the first attempt at IBS-D-targeted drug delivery for improved oral absorption and efficacy through KD-induced target exposure, which holds promising potential for the treatment of IBS-D.

Keywords: irritable bowel syndrome-diarrhea, berberine, microemulsion, ketogenic diet, CB1 receptors

Introduction

Irritable bowel syndrome (IBS) is a prevalent gastrointestinal disease with an overall incidence of 7%–21% worldwide.^{1,2} Among the various subtypes of IBS, irritable bowel syndrome-diarrhea (IBS-D) is one of the most common subtypes,³ accounting for ~35% according to the Rome IV diagnostic criteria. Until now, the pathogenesis of IBS-D has not been entirely understood, but it is related to abnormal signaling of the brain-gut axis,² visceral hypersensitivity,⁴ gastrointestinal (GI) inflammation,⁵ abnormal GI motility,⁶ and imbalance of the gut microbiome.⁷ Among these, the brain-gut axis

as the most concerning area establishes a dialogue channel connecting the central nervous system (CNS) and the GI, involving GI intestinal inflammation, neurotransmitter conduction, anxiety, and depression.⁸ Current clinical strategies are mainly symptomatic drug-based therapies,^{5,9} such as antispasmodics (pinaverium bromide), antidiarrheal drugs (loperamide), intestinal flora changes (ketogenic diet, KD), and antidepressants (paroxetine). Unfortunately, comprehensive drug treatment guidelines have not been established so far.

Berberine (BR), an isoquinoline alkaloid compound, has been used for treating gastroenteritis, dysentery, and enteritis for decades in the clinic.¹⁰ BR was reported to be a potential small-molecule drug for the treatment of IBS-D as it can modulate the release of neurotransmitters.¹¹ However, due to the low solubility, first-pass metabolism, P-glycoprotein (P-gp) efflux, and self-aggregation in the GI, the oral absorption of the BR is poor and limits its clinical application.¹² To enhance the feasibility of IBS-D treatment, designing a rational BR-based oral delivery system is highly desired.

Microemulsion, a nano-sized drug delivery system, is self-assembled by the oil phase, surfactant, and co-surfactant in an aqueous system, with the widely-recognized advantages in solubilization, enhancing oral absorption, and improving stability in vivo.^{13,14} BR has been prepared as the O/W microemulsion, which significantly improved the absorption of BR in the four intestinal segments,¹⁵ creating favorable conditions for various treatments. However, there are two hypotheses needed to be clarified urgently. One is such a simply-encapsulated strategy might be helpful to the treatment of IBS-D; the other one is whether IBS-D-specific drug delivery based on the microemulsion encapsulation could boost its efficacy.

Targeted drug delivery to the desired sites is the primary concern of pharmacists. However, precise drug delivery is challenging for IBS-D, as it lacks exact lesions and targets. The ketogenic diet (KD) is an effective strategy for treating IBS-D through altering the gut microbiota.¹⁶ More notably, IBS-D model rats treated with KD overexpressed cannabidiol receptors (CB receptors) in the gut,¹⁷ which is a promising target for IBS-D-specific delivery of BR. Cannabidiol is a non-psychoactive small-molecule compound, which can not only inhibit neuralgia and reduce inflammation but also has a high affinity with CB1 and CB2 receptors.^{18,19} Therefore, cannabidiol can be used as a potential targeted ligand to help BR achieve IBS-D-targeted drug delivery.

Herein, an amphiphilic material CBD-PEG400 was firstly synthesized and then inserted into the berberine-loaded microemulsion (BR-MEs) to fabricate the CBD-decorated BR-MEs (CBD/BR-MEs). Such a microemulsion system showed high encapsulation efficiency, small particle size, and strong cellular uptake by intestinal cells. With the pretreatment of the KD, the oral absorption of CBD/BR-MEs of the IBS-D model rats was significantly enhanced. The intestinal distribution of CBD/BR-MEs was highly correlated to the intestinal expression of CB1 receptors. Combinational CBD/BR-MEs and KD boosted the comprehensive efficacy of IBS-D models in comparison with the mono CBD/BR-MEs or the free BR treatments. Under the assistance of KD, CBD/BR-MEs interfered with signaling in the gut-brain axis, reduced visceral hypersensitivity, and downregulated the inflammatory cytokines. To the best of our knowledge, our design is the first attempt at IBS-D-targeted delivery of BR, offering promising technologies and ideals for boosting the combinational therapy of IBS-D.

Materials and Methods

Materials

Cannabidiol (CBD) and berberine (BR) were purchased from Nanjing NanoTCM BioTECH Co., Ltd (Jiangsu, China). Kolliphor[®] RH 40 (RH40) and Kolliphor[®] HS15 (HS15) were purchased from BASF Co., Ltd (Shanghai, China). Labrafil M 1944CS was offered by Gattefossé Co., Ltd (Nanterre Cedex, France). Succinic anhydride (SA) was bought from Sigma-Aldrich Co., Ltd. (Poole, UK). Polyethylene glycol 400 (PEG400) was provided by Sinopharm Chemical Reagent Co., Ltd (Shanghai, China). 4-Dimethylaminopyridine (DMAP) and dicyclohexylcarbodiimide (DCC) were purchased from Aladdin Chemical Reagent Co., Ltd (Shanghai, China). Experimental water was produced from the Elix[®]5 Milli Q-water purification system (Millipore, MA, USA). Other chemicals and solvents were used of analytical grade unless otherwise stated.

Synthesis of Cannabidiol-Conjugated PEG400 (CBD-PEG400)

SA (10.0 g, 0.1 mol) and CBD (31.4 g, 0.10 mmol) were dissolved in 150 mL of anhydrous CH_2Cl_2 with DMAP (1.23 g, 0.01 mol) as a catalyst, followed by stirring at room temperature for 24 h.²⁰ After the removal of the solvent, the crude CBD-SA was purified by column chromatography (DCM/MeOH, 30/1, v/v). The synthesise route (Figure S1) was displayed in supporting information. Next, CBD-SA (414 mg, 1 mmol) and PEG400 (380 mg, 0.95 mmol) were dissolved in anhydrous CH_2Cl_2 (50 mL) in an ice water bath. DCC (200 mg, 1 mmol) and DMAP (11 mg, 0.1 mmol) dissolved in 20 mL of anhydrous CH_2Cl_2 were added dropwise to the mixture.²¹ After 24 h of stirring at room temperature, the reaction mixture was filtered and the solvent was removed under the reduced pressure. The crude product (yield, 78.9%) was purified with cold ether thrice. The chemical structure was confirmed by hydrogen nuclear magnetic resonance ($^1\text{H-NMR}$), Fourier-transform infrared (FT-IR), and high-resolution mass spectrometry (HRMS). The synthesise route (Figure S2) was displayed in supporting information.

Preparation of CBD/BR-MEs

CBD/BR-MEs were prepared according to previous reports but with some modifications.²² Briefly, 35 mg of BR, 335 mg of Labrafil M 1944CS, 230 mg of HS15, 250 mg of RH40, 110 mg of PEG400, and 19.6 mg of CBD-PEG400 were strongly stirred at room temperature overnight. Next, 5.0 mL of ultrapure water was added dropwise until the solution was transparent with opalescence. The crude CBD/BR-MEs were purified with a dialysis bag (molecular weight cut off, MWCO, 3000 kDa) for 8 h to obtain CBD/BR-MEs solution.

Characterizations of CBD/BR-MEs

To evaluate encapsulation efficiency (EE) and loading efficiency (LE), CBD/BR-MEs at a total concentration of 2 mg/mL were diluted with 5 volume equivalents of methanol and centrifugated the supernatant, followed by quantifying with high-performance liquid chromatography (HPLC). The EE and LE of BR were calculated by the following equations, respectively.²³

$$\text{EE}(\%) = \frac{W_{(\text{encapsulated drug})}}{W_{(\text{feeding drug})}} \times 100$$

$$\text{LE}(\%) = \frac{W_{(\text{encapsulated drug})}}{W_{(\text{freeze-dried microemulsion})}} \times 100$$

To investigate the centrifugation stability, CBD/BR-MEs were centrifuged at 13,000 g for 10 min, followed by detecting the EE and LE by HPLC. To study the storage stability, CBD/BR-MEs were placed at 25°C for 1 ~ 7 days, and assay the particle size and zeta potential, as well as the EE and LE.

The particle size and zeta potential of the microemulsions were measured by dynamic light scattering (DLS, NanoZS90, Malvern, UK) according to the manipulator protocol. The morphology of the microemulsion was observed by transmission electron microscopy (TEM, Tecnai 12, Netherlands) with the method reported previously. The release profile of BR from the microemulsion was studied according to the previous report. 1 mL of the microemulsion solution placed on a dialysis bag was immersed in 100 mL of artificial intestinal juice (AIJ), artificial gastric juice (AGJ), or phosphate buffer saline (PBS), and stirred at 100 rpm at 37 °C for 48 h. At predetermined time points, 100 μL of the medium was withdrawn to quantify by HPLC. The cumulative release of BR was calculated by the formula as follows.²⁴ Release (%) = $C_{\text{test}} \times 100/50 \times 100\%$, where C_{test} represents the BR content of the sample.

Chromatographic Conditions of BR

BR was determined at 30°C by an Agilent 1260 Infinity instrument (Agilent Technologies Inc., Santa Clara, CA, USA) with an Agilent Zorbax C18 column (250 \times 4.6 mm, 5 μm) eluted with a gradient elution procedure as follows, acetonitrile - 0.1% phosphate buffer (12/88, v/v) from 0 ~ 13 min; acetonitrile - 0.1% phosphate buffer (26/74, v/v) from 13 ~ 28 min. The flow rate was set at 1 mL/min and the detection wavelength was at 345 nm.²⁴

Cell Culture

Caco-2 cells purchased from Biobw BioTech Co., Ltd. (catalog number: bio-69125) were cultured in a cell incubator by using a DMEM medium with fetal bovine serum (FBS, 20%, v%), penicillin (100 IU/mL), and streptomycin (100 µg/mL). The incubator parameters were set as follows, CO₂ atmosphere: 5% and relative humidity: 90%. The culture medium was replaced once cell density reached 60%.

Cytotoxicity of Microemulsions

Five thousand Caco-2 cells seeded in 96-well plates were treated with BR, BR-MEs, and CBD/BR-MEs at BR concentrations ranging from 0.1 ~ 50 µg/mL. After 24 h of the treatments, the cells were stained with MTT solution for 4 h, followed by removing the cell medium and dissolving the resulting formazan crystals with dimethyl sulfoxide (DMSO). The absorbance of each well at 570 nm was recorded using a microplate reader (Varioskan Flash, Thermo). Viability (%) = absorbance of sample/absorbance of control × 100%.

Cellular Uptake

Two hundred thousand Caco-2 cells seeded in 6-well plates were treated with 1.2 mL of BR, BR-MEs, and CBD/BR-MEs at BR concentrations ranging from 10 ~ 50 µg/mL. After 6 h of incubation, the cells were washed with ice-cold PBS thrice, and then prepared 200 µL of single-cell suspension using trypsin solution (Beyotime, Hangzhou, China), followed by extracting the BR with 400 µL of methanol. The cell protein was quantified by the BCA protein kit (Thermo-Fisher, Beijing, China). The cellular uptake (µg/mg) = A_{BR}/A_P , where A_{BR} and A_P represent the amount of intracellular BR and cellular protein, respectively.

Animals

Wistar male rats weighing ~250 g (8 weeks old) were purchased from Speyford (Beijing) Biotechnology Co., Ltd. The rats were fed at the Experimental Animal Center of Jiangsu Province Academy of Traditional Chinese Medicine with an environment of 23 ± 3°C and a humidity of 55 ± 5%. All animal experiments were approved by the Animal Ethics Committee of Jiangsu Province Academy of Traditional Chinese Medicine (AEWC-20220611-212).

Experimental Diets

Diets (standard diet and ketogenic diet) were purchased by Nantong Trophy Feed Technology Co., Ltd (Nantong, China), and administered ad libitum for two weeks before the establishment of the IBS-D model. The composition is shown in Table 1.¹⁷

Establishment of IBS-D Model

After 1 week of acclimation, The IBS-D rats model was established according to the AL-Chaer method but with some modifications.¹⁷ The rats were intragastrically administrated with senna leaf decoction once every day for 14 days. The senna leaf was immersed in 5 times volume of boiling water overnight, filtered, and concentrated to 0.45 g/mL. In addition, the rats were treated with 2 h of restraint stress every day. To verify the IBS-D model, the abdominal withdrawal reflex (AWR) scoring system was used to evaluate visceral hypersensitivity. Bristol scores and fecal water ratio (%) were also employed to evaluate the grades of diarrhea.

Table 1 Composition of the Standard Diet and Ketogenic Diet

Analytical Constituents	Standard Diet	Ketogenic Diet
Moisture	6.8%	0%
Crude protein	12.5%	17%
Crude oils and fats	4%	70%
Crude fibers	6%	6%
Crude ash	3.89%	4%

Pharmacokinetics

The IBS-D model rats were randomly divided into 5 groups ($n = 6$) as follows, (1) CBD/BR-MEs (KD); (2) CBD/BR-MEs; (3) BR-MEs (KD); (4) BR-MEs; (5) BR. All the rats were intragastrically administrated with above-mentioned formulations once at a BR dose of 250 mg/kg. At the predetermined time intervals, 500 μ L of blood was collected from orbital venous plexus. The BR in the plasma was quantified with HPLC, and the main pharmacokinetics indicators were calculated with Kinetica 5.0 software.

Therapeutical Regimen

The rats were randomly divided into 9 groups ($n = 8$) as follows, (1) healthy rats (control); (2) IBS-D (model); (3) CBD/BR-MEs (KD); (4) CBD/BR-MEs; (5) BR-MEs (KD); (6) BR; (7) CBD/MEs (KD); (8) CBD/MEs; (9) KD only. All the rats were intragastrically administrated once every day with different formulations at a BR dose of 250 mg/kg (or a CBD dose of 20 mg/kg) for 14 days after the establishment of the IBS-D model. (KD) represents the rats were pretreated with a KD. During the treatments, the body weight and fecal water (%) were recorded every day.

AWR Scores

The rats fasted 24 h before the test were put into a glass container to restrict their activities. Behavioral responses to various treatments were according to the AL-Chaer method but with some modifications.^{25,26} The standards of an AWR score were determined as follows. AWR 0: normal behavior without any responses; AWR 1: slight head movement once received the stimulus with immobility; AWR 2: abdominal muscles contraction was observed; AWR 3: the abdomen lift off the platform; AWR 4: strong contraction of abdominal muscles with body arching and lifting of pelvic structures.

Bristol Stool Score

The fecal properties of rats were scored according to the Bristol stool form scale.²⁷ The water content of feces before and after the administrations were tested by the following equation, respectively. The water content of rat feces (%) = (mass of fresh feces - mass of dried feces)/mass of fresh feces \times 100%. The dried feces were obtained by drying at 105°C for 8 h.

Immunohistochemistry and Immunofluorescence

The brain and colon tissue of rats treated with different formulations were embedded with paraffin, followed by preparing a 5 μ M-thick section. After standardized dewaxing procedures, the slices were repaired with sodium citrate solution at 120°C for 10 min, sealed with 5% (v/v) BSA for 1 h, and then incubated with different primary antibodies at 4°C overnight. Next, the sections were successively rinsed with PBS thrice, labeled with anti-rabbit IgG, and stained with DAB solution to perform immunohistochemistry studies.²⁸ Likewise, the primary antibody-treated sections were incubated with secondary fluorescence antibodies for 1 h and stained with DAPI at room temperature for 10 min to perform immunofluorescence studies.²⁹ All the sections were immediately observed with an inverted fluorescence microscope (Carl Zeiss, Axiovert 200M, Germany).

Hematoxylin and Eosin Staining

After 24 h of the last administration, the colon tissues of the rats were collected, histologically examined, and fixed in 4% paraformaldehyde for 24 h. Next, the tissues were embedded with paraffin and prepared 5 μ M-thick sections. After standardized dewaxing procedures, the slices were stained with hematoxylin and eosin staining (H&E) and then observed with an optical microscope.

Cytokine Detection

Eight hundred microliters of the blood of the rats were collected after 24 h of the last administration. For cytokine detections, 300 μ L of serum was prepared to detect various cytokines, including calcitonin gene-related peptide (CGRP, Abcam, ab288597), substance P (SP, Abcam, ab240683), serotonin transporter (SERT, 5-HT, Abcam, ab132415), interleukin-1 β (IL-1 β , Abcam, ab197742), interleukin-6 (IL-6, Abcam, ab222503), and tumor necrosis factor- α (TNF-

α , Abcam, ab181421). The detection methods were in accordance with the corresponding manufacturer's protocol of enzyme-linked immunosorbent assay (ELISA) kits.

Systemic Toxicity

At 24 h of the last administration, 100 μ L of blood samples of the rats treated with different formulations were collected for blood routine.³⁰ Likewise, 200 μ L of serum samples were prepared for biochemical tests (Indiko, Thermo-Fisher Scientific, China),³¹ including aspartate transaminase (AST), alanine transaminase (ALT), blood urea nitrogen (BUN), creatinine (CREA), and uric acid (UA).

Statistical Analysis

All data are expressed in mean \pm standard deviation (SD). The statistical difference was compared by Student's *t*-test and ANOVA. * $P < 0.05$ and ** $P < 0.01$ represent significant and extremely significant differences, respectively. All analyses were performed by using GraphPad 8.0 (GraphPad Software, Inc.).

Results and Discussion

Synthesis and Chemical Characterizations of CBD-PEG400

To modify the BR-MEs with CBD, CBD-PEG400 was synthesized by connecting PEG400 and CBD using succinic anhydride as a linker. According to the ¹H-NMR spectrum displayed in [Figure S3](#), the intensive signals between δ (ppm) 3.58 ~ 3.92 ppm were attributed to the PEG segments. The triple peaks at δ (ppm) 2.08 and 2.46 belonged to the linker. The characteristic chemical shift at δ (ppm) 5.80 ~ 6.26 was attributed to the hydrogens of the CBD aromatic ring. The aliphatic chain hydrogen peaks belonging to CBD at δ (ppm) 0.83 ~ 0.98 were also observed. The HRMS result presented the molecular weight at 752.4267 ± 44 x, which is a typical molecular weight of the PEG derivatives ([Figure S4](#)). Additionally, the characteristic absorption peaks attributed to the succinic linker (1733.7 cm^{-1} , ester bonds), PEG segments (1298.0 , 1249.3 , and 1106.7 cm^{-1}), and CBD segments (1375.5 , 2874.4 cm^{-1} , the aliphatic chain; 1621.7 cm^{-1} , the vinyl; 1642.9 cm^{-1} , the aromatic ring) were observed from the FT-IR spectrum, respectively ([Figure S5](#)). All these results indicate the successful synthesis of CBD-PEG400.

Preparation and Characterizations of CBD/BR-MEs

Based on our previous studies,³² we determined the weight ratio of the oil phase to the surfactant at $\sim 1/2$ and the K_m value at $3/1$, as these parameters were suitable for the formation of the microemulsion. In this section, the effects of introducing CBD-PEG400 on the formation of the microemulsion were investigated. As shown in the pseudo-ternary phase diagram ([Figure 1A](#)), the microemulsion areas of various groups did not differ significantly after adding 0.5% ~ 2.7% (wt%) CBD-PEG400. Furthermore, the particle size and transmittance of the CBD-decorated blank microemulsions (CBD/MEs) ([Figure 1B](#)) were not significantly affected when the added CBD-PEG400 was not greater than 2% (wt%). To ensure the sufficient density of CBD and smaller size, 2.0% (wt%) CBD-PEG400 was introduced into the microemulsion. After encapsulating BR, CBD/BR-MEs exhibited an approximately spherical shape with a particle size of ~ 33 nm ([Figure 1C](#)), similar to CBD/MEs and BR-MEs, indicating that BR encapsulation and CBD modification have little effect on particle size. The EE was beyond 80% until overloading (30% feeding, [Figure 1D](#)) and the LE of BR increased with feeding until reaching 30% ([Figure 1E](#)). CBD/BR-MEs released $75.5 \pm 4.6\%$ BR at the AGJ within 48 h, which is significantly faster than that at the AIJ ($48.9 \pm 3.9\%$, [Figure 1F](#)). Such accelerated drug release of microemulsions at acidic pH is consistent with previously reported literature.²²

Cellular Studies

To investigate the safety of the formulations toward normal intestinal cells, the potential cytotoxicity of the BR-based formulations was studied. As shown in [Figure 2A](#), CBD/BR-MEs at a BR concentration below 50 μ g/mL did not inhibit the growth of Caco-2 cells. Likewise, the free BR and BR-MEs were both noncytotoxic toward Caco-2 cells at the BR concentrations ranging from 0.1 ~ 50 μ g/mL. To verify whether the microemulsion system could promote the

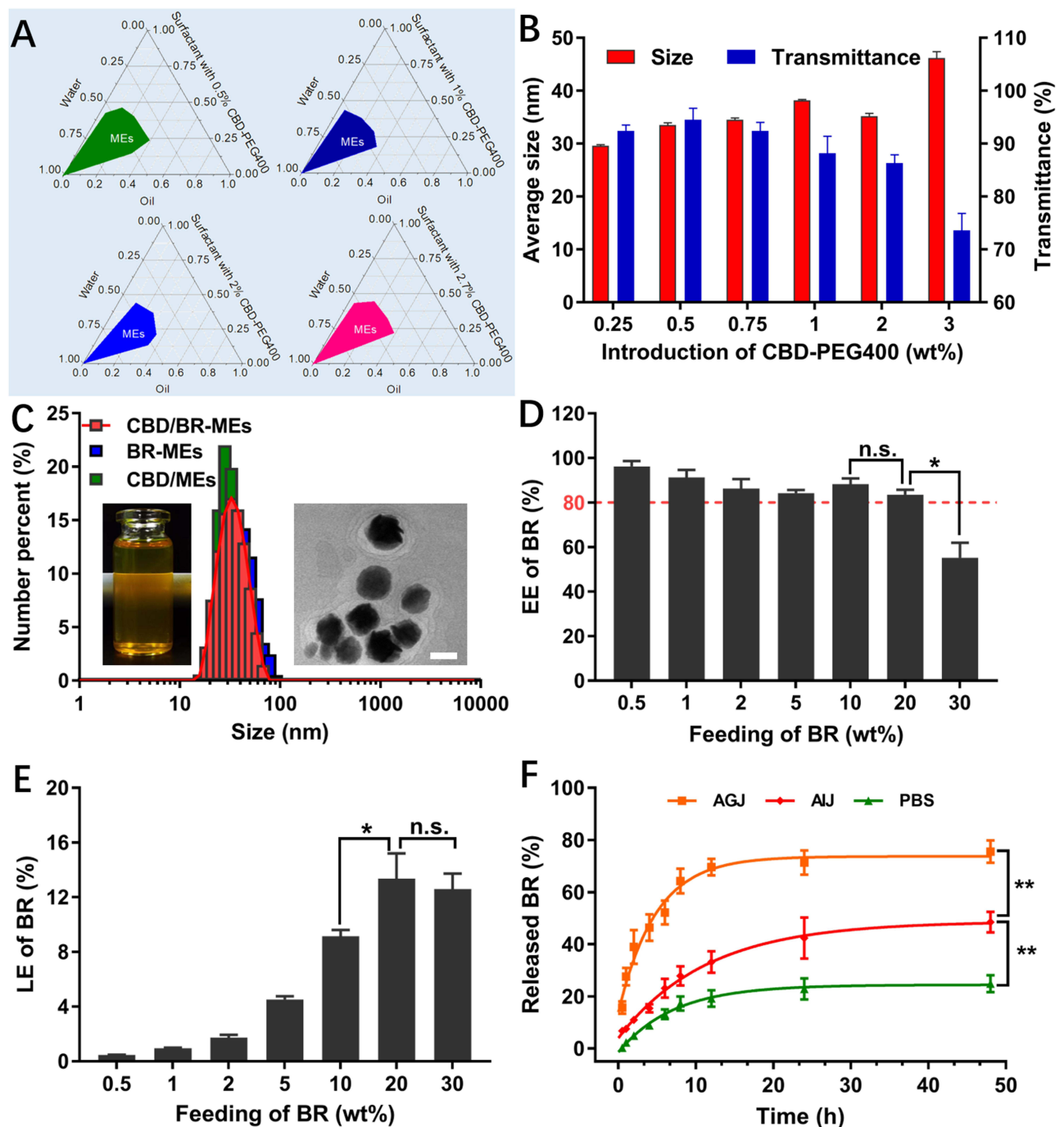


Figure 1 Preparation and characterizations of CBD/BR-MEs. (A) Pseudo-ternary phase diagram of CBD/BR-MEs incorporating a different amount of CBD-PEG400. (B) Effects of CBD-PEG400 introduction on particle size and transmittance of CBD/BR-MEs. (C) DLS analysis of the microemulsions. The inserted pictures (left) and (right) are CBD/BR-MEs solution and its TEM image, respectively. The bar is 50 nm. (D) EE and (E) LE of BR from CBD/BR-MEs with different feeding of BR. Data are represented as mean \pm SD, $n = 4$. * $P < 0.05$. The EE above the red dash line ($>80\%$) represents a good encapsulation. (F) Release profile of BR from CBD/BR-MEs at different mediums within 48 h. Data are represented as mean \pm SD, $n = 6$. ** $P < 0.01$.

internalization of BR, the cellular uptake of BR, BR-MEs, and CBD/BR-MEs were investigated. As exhibited in Figure 2B, the cellular uptake of BR-MEs was significantly higher than that of BR at the three observed concentrations. CBD/BR-MEs did not further increase the internalization based on BR-MEs. These results suggest that CBD/BR-MEs are safe and capable of increasing the cellular uptake of free BR, but the modification of CBD did not promote the uptake of normal intestinal cells.

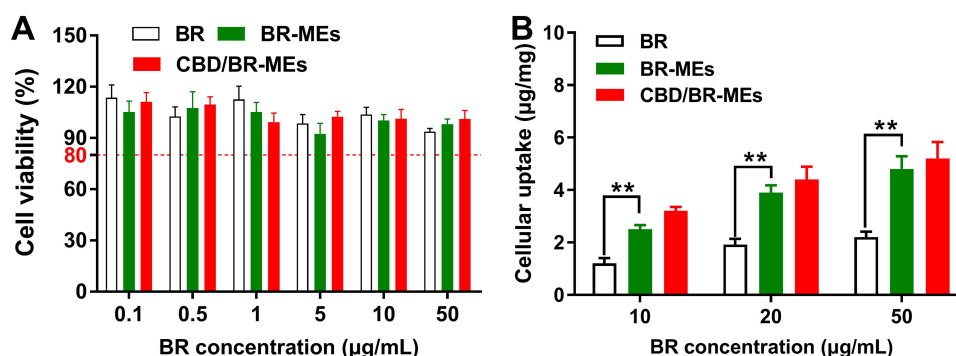


Figure 2 Cellular studies. **(A)** Cytotoxicity of various formulations against Caco-2 cells. The cell viability above the red dash line (>80%) represents a good safety toward the cells. **(B)** Cellular uptake of BR after Caco-2 cells were treated with different formulations at the BR concentration ranging from 10 ~ 50 µg/mL for 6 h. Data are represented as mean ± SD, n = 4. ***p* < 0.01.

Pharmacokinetics

According to our design, IBS-D model rats fed the KD overexpressed CB1 receptors, which could be used for targeted BR delivery and enhanced intestinal absorption. In this part, the pharmacokinetics of the microemulsions with or without the KD were studied and compared in the IBS-D model rats. As shown in Figure 3, the average plasma BR concentration of all four microemulsions was significantly higher than that of the free BR, suggesting that the microemulsion system is favorable to intestinal absorption.³³ As expected, after the administration of CBD/BR-MEs, the concentration of BR in the plasma of rats fed a KD was significantly higher than that of standard diet-fed rats. Notably, the presence of KD did not change the oral absorption of BR-MEs. As presented in Table 2, The AUC and C_{max} of CBD/BR-MEs with a KD were 1.71 times and 1.47 times that with the standard diet, respectively. Such a trend was also observed in $t_{1/2}$ and MRT, further validating that KD-resulted CB-1 receptor overexpression promotes the oral absorption of CBD/BR-MEs. The main pharmacokinetic parameters of BR-MEs were comparable regardless of whether the rats were fed a KD or not. These results suggested that CBD modification and microemulsion encapsulation are two critical factors for enhancing the oral absorption of CBD/BR-MEs in KD-fed rats.

Intestinal CB1 Expression and Microemulsions Distribution

In this part, C6-labeled microemulsions were utilized to further validate that KD-induced CB1 receptors overexpression in the intestine of IBS-D model rats improved the absorption of CBD/C6-MEs. As shown in Figure 4A and B, the red fluorescence (CB1 receptors) in the intestine of the KD-treated rats was significantly stronger than that of the IBS-D model rats, which is in agreement with a previous report.¹⁷ The colocalization coefficient of CBD/C6-MEs (KD) group reached about 0.432, which is significantly higher than that of C6-MEs (KD) group (0.072). The distribution profiles of C6-MEs had no significant differences between the

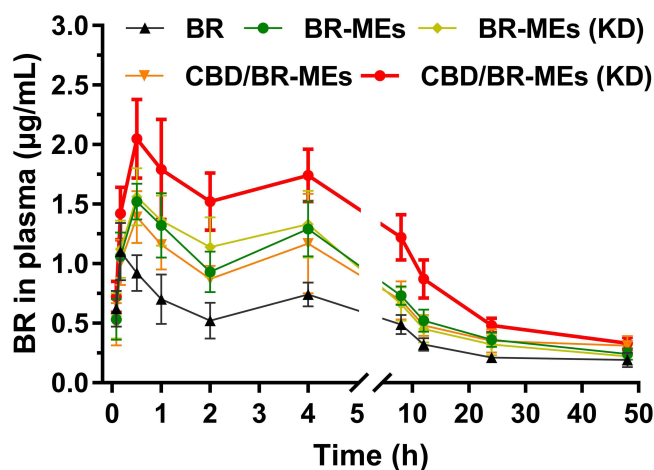


Figure 3 BR concentration-time curve of the plasma after the rats orally-administrated with different formulations at a BR dose of 250 mg/kg within 48 h. Data are represented as mean ± SD, n = 6.

Table 2 Pharmacokinetic Parameters of Various BR Formulations After I.g. Administration at a BR Dose of 250 Mg/Kg

Parameter	BR	BR-MEs	BR-MEs (KD)	CBD/BR-MEs	CBD/BR-MEs (KD)
AUC _{0-∞} (μg/mL/h) ^a	10.52 ± 2.16	17.78 ± 3.18**	16.35 ± 3.67**	15.99 ± 3.26**	27.42 ± 6.25*##&&
t _{max} (h) ^b	0.48 ± 0.12	0.68 ± 0.29 **	0.71 ± 0.27**	0.63 ± 0.33 *	1.21 ± 0.27 *##&&
t _{1/2} (h) ^c	21.15 ± 3.52	27.38 ± 3.34**	29.13 ± 3.42**	25.44 ± 4.04*	37.62 ± 4.17*##&&
C _{max} (μg/mL) ^d	1.10 ± 0.14	1.52 ± 0.15**	1.56 ± 0.24**	1.39 ± 0.22	2.05 ± 0.33*##&&
MRT _{0-∞} (h) ^e	29.42 ± 2.16	36.24 ± 4.97	39.73 ± 3.52*	40.16 ± 5.47**	52.66 ± 6.24*##&&

Notes: ^a AUC_{0-∞}, area under the plasma concentration-time curve; ^b t_{max}, time of maximum concentration; ^c t_{1/2}, elimination half-life; ^d C_{max}, maximum concentration; ^e MRT_{0-∞}, mean residence time. Data are represented as mean ± SD, n = 6. Compared with BR, *P < 0.05, **P < 0.01; compared with BR-MEs (KD), ##P < 0.01; compared with CBD/BR-MEs, &P < 0.05; &&P < 0.01.

KD-fed and standard diet-fed model rats. As expected, the combinational CBD/C6-MEs and KD presented overwhelming green fluorescence in the intestine among all the treatments (Figure 4A and C), further suggesting that KD-induced CB1 overexpression indeed increases the oral absorption of CBD/C6-MEs. These results also indirectly verify the rationality of the pharmacokinetics behaviors.

Anti IBS-D Efficacy

As shown in Figure 5A, there was no significant difference in body weight after all treatments, indicating acceptable systemic safety. The fecal water content of the KD-fed rats treated with CBD/BR-MEs was significantly lower than the

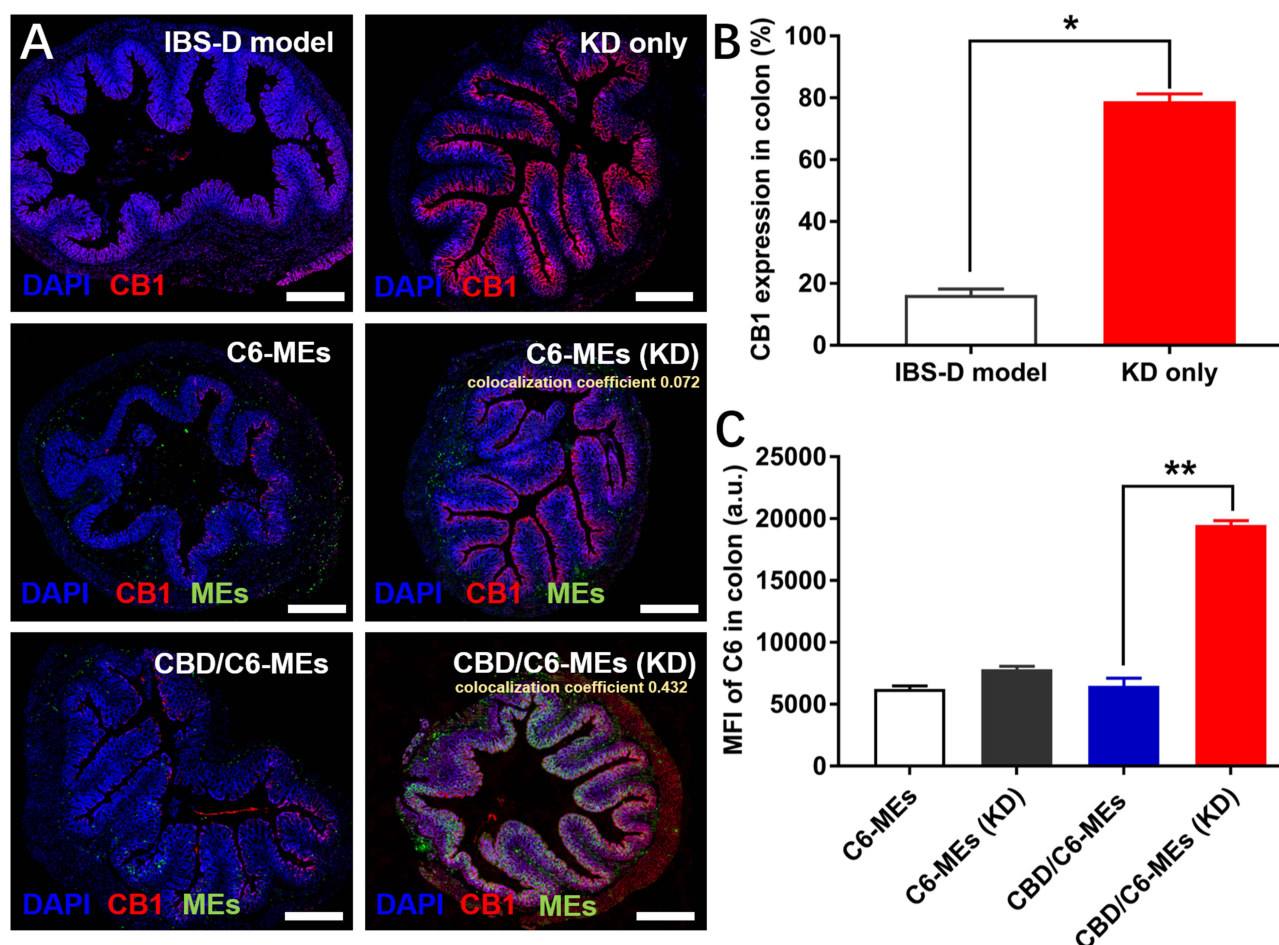


Figure 4 (A) Immunofluorescence staining of CB-1 receptors (red), C6-labeled microemulsions (green), and DAPI (blue, nucleus) of intestinal sections. The bar is 500 μm. The colocalization coefficient of the red and green signal was displayed in the C6-MEs and CBD/C6-MEs groups. (B) Expression of CB-1 in 5 randomly-selected randomly-selected field of views (FOVs). (C) MFI of C6 in 5 randomly-selected FOVs. Data are represented as mean ± SD, n = 5. *P < 0.05, **P < 0.01. Quantification was calculated by ImageJ software.

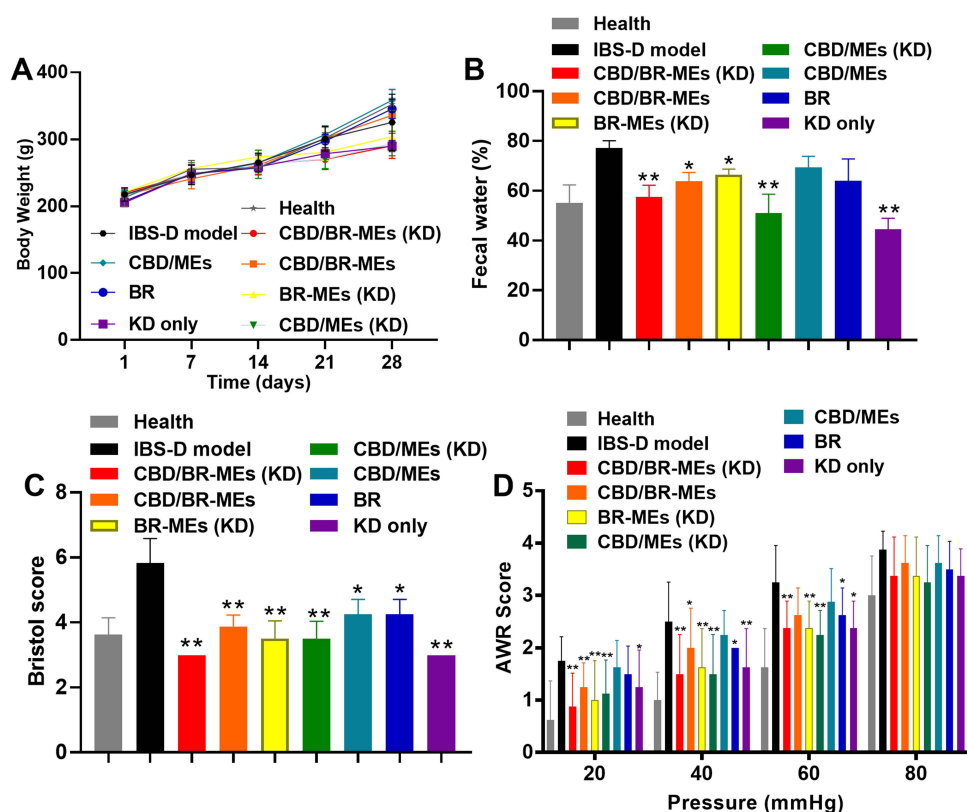


Figure 5 (A) Body weight of rats during and after the treatments. Data are represented as mean \pm SD, $n = 8$. (B) Fecal water ratio after different treatments. Data are represented as mean \pm SD, $n = 8$. * $P < 0.05$, ** $P < 0.01$, compared with the IBS-D model. (C) Bristol stool score of rats after different treatments. Data are represented as mean \pm SD, $n = 8$. * $P < 0.05$, ** $P < 0.01$, compared with the IBS-D model. (D) AWR score of treated-rats receiving the stimulations of 20 ~ 80 mmHg pressure. Data are represented as mean \pm SD, $n = 8$. * $P < 0.05$, ** $P < 0.01$, compared with the IBS-D model.

IBS-D models (Figure 5B). An obvious decrease in fecal water ratio was also observed after treatments of CBD/BR-MEs and the other three KD-involved. According to the form of feces, the Bristol stool scale was used to score the animal stool after the treatments. As exhibited in Figure 5C, the Bristol score of CBD/BR-MEs (KD)-treated rats was the lowest among all the treatments. Notably, the treatments with CBD/MEs (KD) not only reduced fecal water ratio but also lowered the Bristol score, indicating that CBD-PEG400 probably has potential in treating IBS-D under the premise of sufficient intestinal absorption. The AWR scoring system mainly used to evaluate visceral hypersensitivity is an important indicator for the efficacy of IBS-D therapy. Figure 5D demonstrated that CBD/BR-MEs (KD)-treated rats had a remarkably lower score than the IBS-D model rats under the stimulations of 20 ~ 60 mmHg pressure. Without synergistic treatment of KD, the AWR scores of CBD/BR-MEs were increased. All KD-involved treatments were capable of reducing the AWR scores in comparison with the IBS-D model. The mono treatment of CBD/MEs is ineffective for visceral hypersensitivity, which might be associated with insufficient oral absorption. These results suggest that combinational CBD/BR-MEs and KD can collaboratively improve anti-IBS-D efficacy, with one of the potential mechanisms being relative to the IBS-D-targeted delivery of BR.

Intestinal Permeability

Increased intestinal permeability has been considered one of the most potential pathophysiological mechanisms of IBS-D. A large amount of clinical evidence demonstrated that IBS-D patients with impaired epithelial barrier function had the risk of various pathogens or toxins invasion through the intestinal mucosa, resulting in a series of digestive symptoms. ZO-1 (zonula occludens-1) is one of the most well-studied tight junction proteins, whose expression is highly correlated with intestinal permeability. As shown in Figure 6A and B, the total expression of ZO-1 in the intestines of IBS-D model rats was significantly reduced compared with that in the healthy rats. After the treatment of CBD/BR-MEs, the ZO-1 expression was upregulated and obviously higher than the CBD/MEs and BR group, which is probably associated with the microemulsion-enhanced BR intestinal absorption. Notably,

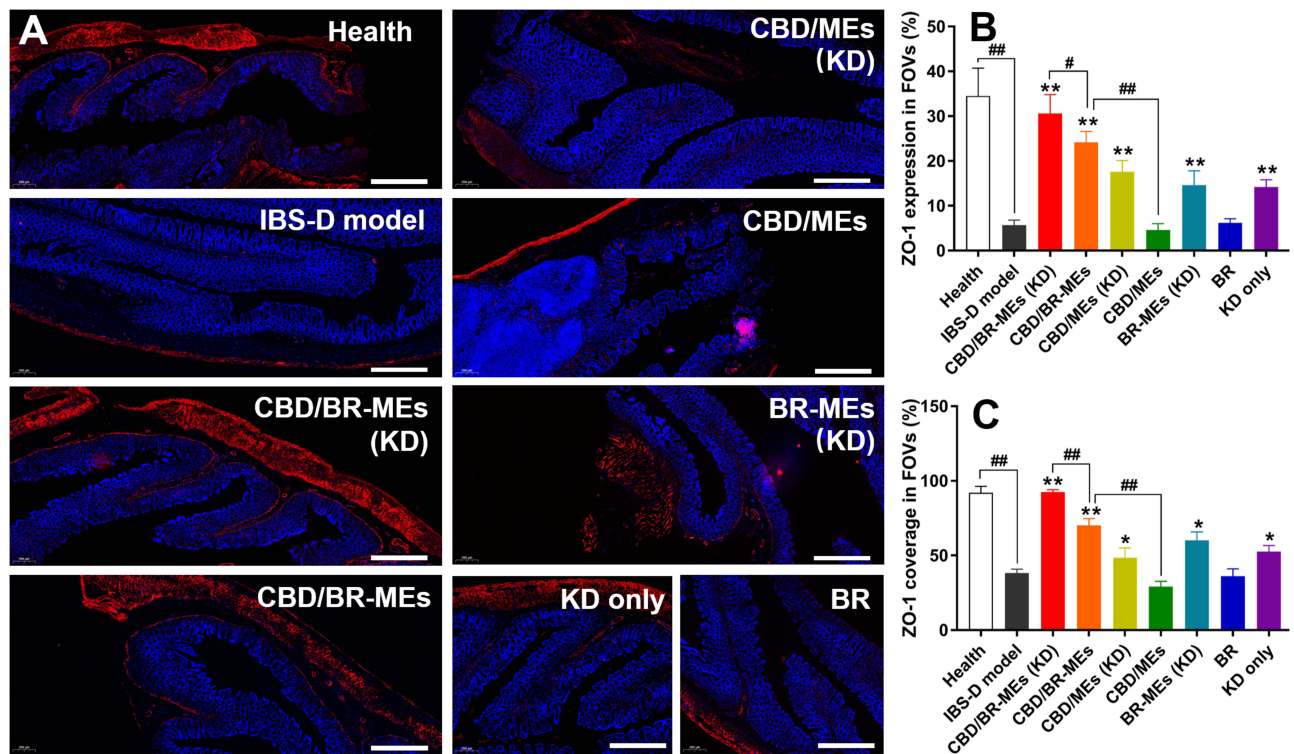


Figure 6 Studies of intestinal permeability. (A) Immunofluorescence staining of ZO-1. The bar is 500 μ m. (B) Expression of ZO-1 in 5 randomly-selected FOVs. (C) Coverage ratio of ZO-1 in 5 randomly-selected FOVs. Data are represented as mean \pm SD, $n = 5$. * $P < 0.05$, ** $P < 0.01$, compared with the IBS-D model; # $P < 0.05$, ### $P < 0.01$. Quantification was calculated by ImageJ software.

CBD/BR-MEs with KD can further increase the expression of ZO-1. Besides, all the treatments with KD were capable of increasing ZO-1 expression to some extent. These results suggest that KD and CBD/BR-MEs synergistically reduce intestinal permeability. We also evaluated the intestinal permeability by quantifying ZO-1 coverage (Figure 6C), the CBD/BR-MEs (KD) group showed an overwhelming fluorescence coverage ratio among all the groups. Without assistance from the KD, ZO-1 coverage in the CBD/BR-MEs group significantly dropped, but it was still higher than the CBD/MEs and BR group. The obtained results demonstrate that the microemulsion encapsulation and KD can synergistically help BR to reduce intestinal permeability.

CREB/BDNF/c-Fos Signaling in the Brain

The previous report has demonstrated a crosstalk mechanism between the GI tract and the CNS.³⁴ CREB is an important transcriptional regulator involved in the regulation of pain pathway signaling. BDNF, widely expressed in the brain, supports and nourishes neurons in the CNS; however, it can cause intestinal hypersensitivity and promote intestinal motility once the expression is abnormally elevated. Changes in these markers might affect pain transmission in the gut, leading to the symptoms of IBS-D. The high expression of c-Fos in the brain has been considered closely related to visceral hypersensitivity in IBS-D patients.³⁵ In view of this, the effects of combinational CBD/BR-MEs and KD on the CREB/BDNF/c-Fos signaling³⁶ in the brain were investigated. As shown in Figure 7A, the IBS-D model rats exhibited stronger c-Fos fluorescence than the healthy rats. The mono treatment with the KD did not significantly decrease the level of c-Fos in comparison with the health group. Combinational treatment with CBD/BR-MEs and KD remarkably reduced the expression of c-Fos, and such a phenomenon was also observed in the CBD/MEs (KD) and CBD/BR-MEs groups. However, neither CBD/MEs nor BR-MEs (KD) lowered the expression of c-Fos (Figure S6). As shown in Figure 7B, the CREB fluorescence in the brain sections of the IBS-D model was obviously stronger than that of the healthy rats. The treatment with CBD/BR-MEs (KD) displayed the lowest CREB signal among all the groups. CBD/BR-MEs, CBD/MEs (KD), and KD alone could also downregulate the level of CREB. According to the BDNF-IHC images (Figure 7C), the positive signal from the CBD/BR-MEs (KD)-treated brain sections was the weakest compared with the other groups. It is worth noting that both CBD modification and the KD contribute to hindering the CREB/BDNF/c-Fos signaling. These results indicate

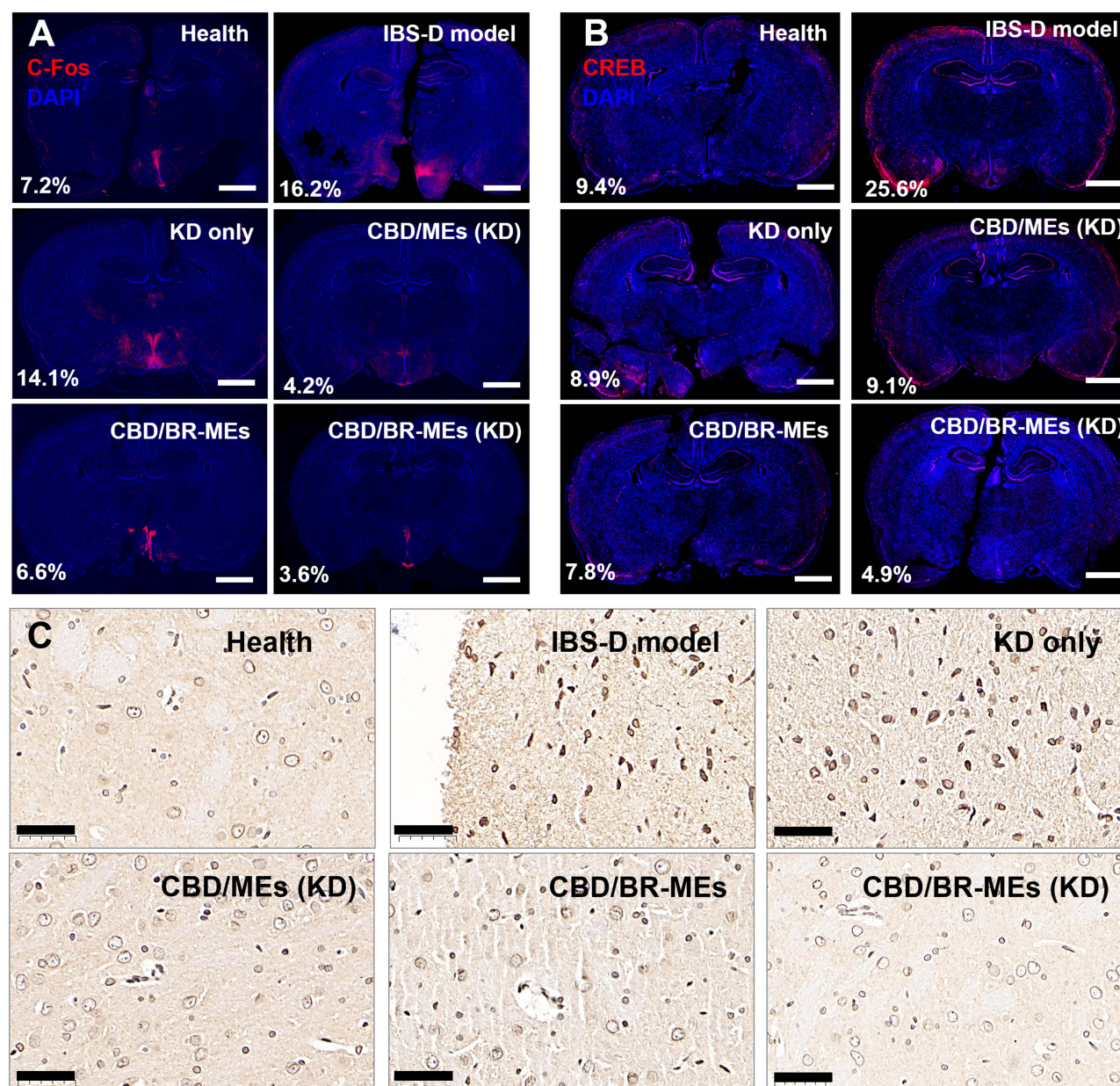


Figure 7 Immunofluorescence staining of (A) c-Fos and (B) CREB in the brain sections. The bar is 2000 μm for (A and B). Quantification displayed at the lower right was calculated by ImageJ software. (C) IHC-stained BDNF images of the brain sections after the rats treated with different formulations. The bar is 200 μm .

that CBD/BR-MEs (KD) might reduce the visceral hypersensitivity of the IBS-D models by blocking the CREB/BDNF/c-Fos signaling in the CNS.

ELISA Tests

According to the previous report, IBS-D is not only a chronic intestinal disorder but also an enteric neurosis, which is associated with some psychological disorders, such as generalized anxiety, depression, and panic.³⁷ In this part, some neurotrophic factors, neurotransmitters, and inflammatory cytokines were monitored to evaluate the influences of the treatments on the brain-gut axis. SP has the effects of enhancing gastrointestinal motility, increasing gastrointestinal smooth muscle contraction, stimulating intestinal mucosal vasodilation, and promoting intestinal secretion of water and electrolytes. As shown in Figure 8A, the SP concentration in the serum of rats treated with CBD/BR-MEs (KD) was significantly lower than the IBS-D model, which is helpful to reduce diarrhea and abdominal pain. CGRP can alter visceral sensory transduction signals via changing blood flow,

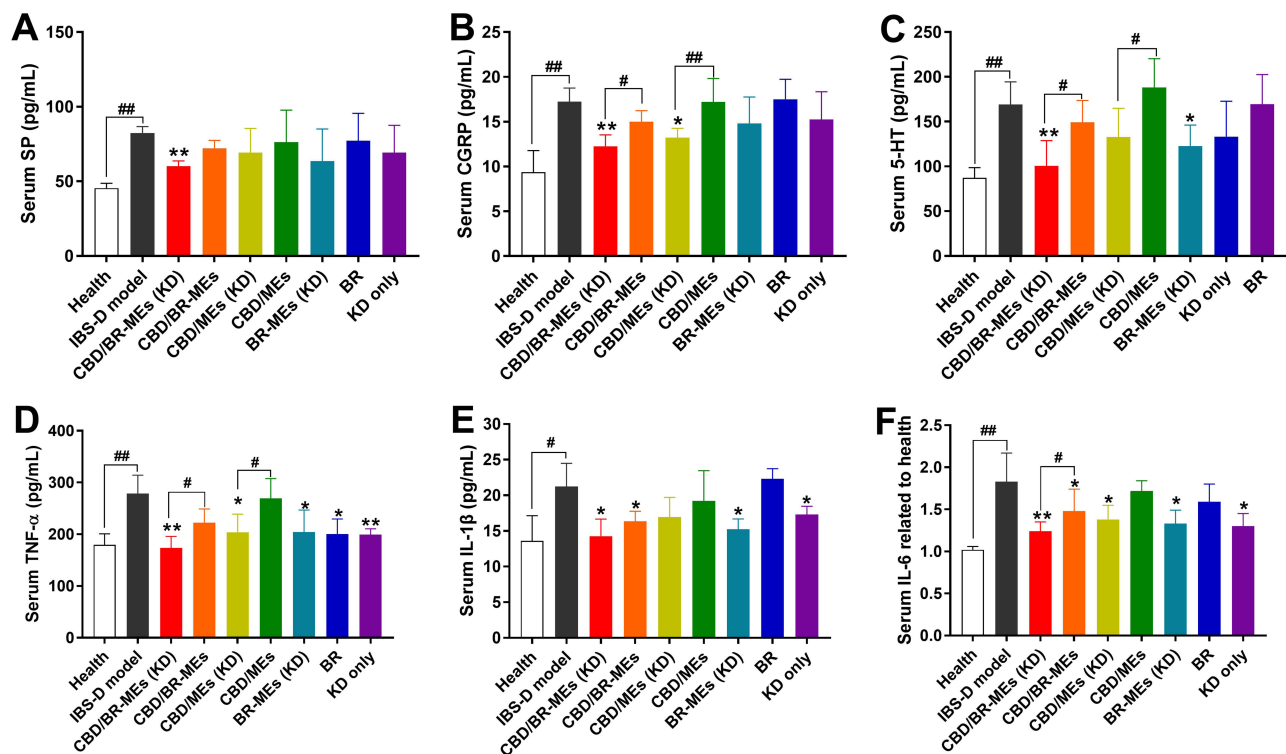


Figure 8 Serum concentration of (A) SP, (B) CGRP, (C) 5-HT, (D) TNF- α , (E) IL-1 β , and (F) IL-6 after the treatments. Data are represented as mean \pm SD, $n = 8$. * $P < 0.05$, ** $P < 0.01$, compared with the IBS-D model. ### $P < 0.01$; # $P < 0.05$.

regulating smooth muscle contraction, and mediating pain transduction, which also might be associated with abnormal gastrointestinal motility and abdominal pain. As shown in Figure 8B, the treatment of CBD/BR-MEs (KD) remarkably downregulated the serum CGRP in comparison with that of CBD/BR-MEs alone. Besides, the treatment of CBD/MEs (KD) also decreased the level of serum CGRP compared with CBD/MEs alone. 5-HT is one of the neurotransmitters involved in the regulation of visceral sensation, smooth muscle tension, and gastrointestinal contraction. An increased 5-HT commonly observed in IBS-D patients is also accompanied by the promotion of intestinal peristalsis and elevation of visceral sensitivity. As shown in Figure 8C, the serum 5-HT concentration tested for the CBD/BR-MEs (KD) group was significantly lower than the IBS-D model, as well as the CBD/BR-MEs alone. Furthermore, the CBD/BR-MEs (KD) group also notably reduced the serum TNF- α , IL-1 β , and IL-6 compared with the model rats (Figure 8D-F). The KD can not only alone but also synergistically downregulate the levels of inflammatory cytokines with CBD/BR-MEs. All the BR-loaded microemulsions demonstrated some anti-inflammatory effects to varying degrees. These results suggest that combinational CBD/BR-MEs and KD possessed the advantages over mono CBD/BR-MEs in reducing intestinal smooth muscle contraction, blocking pain signaling, and downregulating the level of inflammatory cytokines. More importantly, the boosted BR delivery to the IBS-D area might be a potential reason for the enhanced efficacy.

Safety Evaluation

After 14 days of the treatments, CBD/MEs, BR-MEs, and CBD/BR-MEs did not lead to any damage against the kidney or liver of the rats. There were no significant differences in biochemical indicators between the treated and non-treated rats (Figure S7). The blood routine analysis demonstrated no obvious abnormality among all the treatments (Figure S8). Besides, no obvious lesions or inflammation sites were observed from all the HE-stained intestinal sections (Figure S9). These results suggest that oral administration of CBD/BR-MEs for IBS-D therapy has acceptable safety *in vivo*.

Conclusion

In summary, CBD/BR-MEs were successfully fabricated to enhance oral absorption and treat IBS-D. The pharmacokinetic performance of the treatment with CBD/BR-MEs was significantly improved with the assistance of KD-induced overexpression

of CB1 receptors. The combination of CBD/BR-MEs and KD demonstrated stronger anti-IBS-D efficacy compared to CBD/BR-MEs alone. CBD/BR-MEs (KD) not only reduced intestinal permeability but also blocked the CREB/BDNF/c-Fos signaling pathway associated with visceral hypersensitivity. Additionally, CBD/BR-MEs (KD) decreased serum levels of neurotrophic factors, neurotransmitters, and inflammatory cytokines in IBS-D model rats. The CBD modification and microemulsion system are both crucial contributors to the boosted IBS-D therapy. The design of CBD/BR-MEs and the combinational therapy with KD provide promising strategies for treating IBS-D.

Data Sharing Statement

All data presented in this paper are included in the main text and the supplementary information.

Ethics Approval and Consent to Participate

All animals were treated in accordance with the Guide for Care and Use of Laboratory Animals published by the Animal Ethics Committee of Jiangsu Province Academy of Traditional Chinese Medicine.

Consent for Publication

All authors of this study agreed to publish.

Acknowledgments

This work was supported by National Natural Science Foundation of China (82173980 and 81873017), Natural Science Foundation of Jiangsu Province of China (BK20211389), the Six Talent Peak Project of Jiangsu Province (WSN-040; YY-028-2019), and the Jiangsu Provincial Cadre Health Research Project (BJ20026).

Funding

This work was also supported by Graduate Research and Practice Innovation Project of Jiangsu Province (SJCX22-0841).

Disclosure

No potential conflict of interest was reported by the authors.

References

1. Chey WD, Kurlander J, Eswaran S. Irritable bowel syndrome: a clinical review. *JAMA*. 2015;313(9):949–958. doi:10.1001/jama.2015.0954
2. Enck P, Aziz Q, Barbara G, et al. Irritable bowel syndrome. *Nat Rev Dis Primers*. 2016;2:16014. doi:10.1038/nrdp.2016.14
3. Singh P, Staller K, Barshop K, et al. Patients with irritable bowel syndrome-diarrhea have lower disease-specific quality of life than irritable bowel syndrome-constipation. *World J Gastroenterol*. 2015;21(26):8103–8109. doi:10.3748/wjg.v21.i26.8103
4. Gracie DJ, Hamlin PJ, Ford AC. The influence of the brain-gut axis in inflammatory bowel disease and possible implications for treatment. *lancet Gastroenterol Hepatol*. 2019;4(8):632–642. doi:10.1016/S2468-1253(19)30089-5
5. Shi C, Dawulieti J, Shi F, et al. A nanoparticulate dual scavenger for targeted therapy of inflammatory bowel disease. *Sci Adv*. 2022;8(4):eabj2372.
6. Barbaro MR, Cremon C. Non-Celiac Gluten Sensitivity in the Context of Functional Gastrointestinal Disorders. *Nutrients*. 2020;12(12):3735. doi:10.3390/nu12123735
7. Martin CR, Osadchiv V, Kalani A, Mayer EA. The Brain-Gut-Microbiome Axis. *Cell Mol Gastroenterol Hepatol*. 2018;6(2):133–148. doi:10.1016/j.jcmgh.2018.04.003
8. Pinto-Sanchez MI, Hall GB, Ghajar K, et al. Probiotic Bifidobacterium longum NCC3001 Reduces Depression Scores and Alters Brain Activity: a Pilot Study in Patients With Irritable Bowel Syndrome. *Gastroenterology*. 2017;153(2):448–459. doi:10.1053/j.gastro.2017.05.003
9. Xu J, Xu J, Shi T, et al. Restores Intestinal Homeostasis in Colitis by Regulating Redox Balance, Immune Responses, and the Gut Microbiome. *Adv Mater*. 2023;35(3):e2207890. doi:10.1002/adma.202207890
10. Zhang W, Xu JH, Yu T, Chen QK. Effects of berberine and metformin on intestinal inflammation and gut microbiome composition in db/db mice. *Biomed Pharmacother*. 2019;118:109131. doi:10.1016/j.biopha.2019.109131
11. Lu Y, Huang J, Zhang Y, et al. Therapeutic Effects of Berberine Hydrochloride on Stress-Induced Diarrhea-Predominant Irritable Bowel Syndrome Rats by Inhibiting Neurotransmission in Colonic Smooth Muscle. *Front Pharmacol*. 2021;12:596686. doi:10.3389/fphar.2021.596686
12. Wang Y, Tong Q, Ma SR, et al. Oral berberine improves brain dopa/dopamine levels to ameliorate Parkinson's disease by regulating gut microbiota. *Signal Transduction and Targeted Therapy*. 2021;6(1):77. doi:10.1038/s41392-020-00456-5
13. Qu D, Wang L, Qin Y, et al. Non-triggered sequential-release liposomes enhance anti-breast cancer efficacy of STS and celastrol-based microemulsion. *Biomaterials sci*. 2018;6(12):3284–3299. doi:10.1039/C8BM00796A

14. Su X, Gao C, Shi F, et al. A microemulsion co-loaded with Schizandrin A-docetaxel enhances esophageal carcinoma treatment through overcoming multidrug resistance. *Drug Deliv.* **2017**;24(1):10–19. doi:10.1080/10717544.2016.1225854
15. Gui SY, Wu L, Peng DY, Liu QY, Yin BP, Shen JZ. Preparation and evaluation of a microemulsion for oral delivery of berberine. *Die Pharmazie.* **2008**;63(7):516–519.
16. Ang QY, Alexander M, Newman JC, et al. Ketogenic Diets Alter the Gut Microbiome Resulting in Decreased Intestinal Th17 Cells. *Cell.* **2020**;181(6):1263–1275. doi:10.1016/j.cell.2020.04.027
17. Gigante I, Tutino V, Russo F. Cannabinoid Receptors Overexpression in a Rat Model of Irritable Bowel Syndrome (IBS) after Treatment with a Ketogenic Diet. *International Journal of Molecular Sciences.* **2021**;22(6):2880. doi:10.3390/ijms22062880
18. Laprairie RB, Bagher AM, Kelly ME, Denovan-Wright EM. Cannabidiol is a negative allosteric modulator of the cannabinoid CB1 receptor. *Br J Pharmacol.* **2015**;172(20):4790–4805. doi:10.1111/bph.13250
19. Pertwee RG. The diverse CB1 and CB2 receptor pharmacology of three plant cannabinoids: delta9-tetrahydrocannabinol, cannabidiol and delta9-tetrahydrocannabivarin. *Br J Pharmacol.* **2008**;153(2):199–215. doi:10.1038/sj.bjp.0707442
20. Fathalipour S, Ataei B, Janati F. Aqueous suspension of biocompatible reduced graphene oxide- Au NPs composite as an effective recyclable catalyst in a Betti reaction. *Mater Sci Eng C Mater Biol Appl.* **2019**;97:356–366. doi:10.1016/j.msec.2018.12.048
21. Zhong L, Xu L, Liu Y, et al. Transformative hyaluronic acid-based active targeting supramolecular nanoplateform improves long circulation and enhances cellular uptake in cancer therapy. *Acta pharmaceutica Sinica B.* **2019**;9(2):397–409. doi:10.1016/j.apsb.2018.11.006
22. Zuo Z, Li M, Han T, et al. A platelet-cloaking tetramethylpyrazine-loaded microemulsion for improved therapy of myocardial ischaemia/reperfusion injury. *J Drug Target.* **2022**;30(6):646–656. doi:10.1080/1061186X.2022.2048389
23. Chen Y, Wang S, Hu Q, Zhou L. Self-Emulsifying System Coloaded with Paclitaxel and Coix Seed Oil Deeply Penetrated to Enhance Efficacy of Cervical Cancer. *Curr Drug Deliv.* **2022**;2:56.
24. Maulvi FA, Desai AR, Choksi HH, et al. Effect of surfactant chain length on drug release kinetics from microemulsion-laden contact lenses. *Int J Pharm.* **2017**;524(1–2):193–204. doi:10.1016/j.ijpharm.2017.03.083
25. Bao CH, Wang CY, Li GN, et al. Effect of mild moxibustion on intestinal microbiota and NLRP6 inflammasome signaling in rats with post-inflammatory irritable bowel syndrome. *World J Gastroenterol.* **2019**;25(32):4696–4714. doi:10.3748/wjg.v25.i32.4696
26. Al-Chaer ED, Kawasaki M, Pasricha PJ. A new model of chronic visceral hypersensitivity in adult rats induced by colon irritation during postnatal development. *Gastroenterology.* **2000**;119(5):1276–1285. doi:10.1053/gast.2000.19576
27. Zhou Q, Verne ML, Fields JZ, et al. Randomised placebo-controlled trial of dietary glutamine supplements for postinfectious irritable bowel syndrome. *Gut.* **2019**;68(6):996–1002. doi:10.1136/gutjnl-2017-315136
28. Pleguezuelos-Manzano C, Puschhof J, van den Brink S, Geurts V, Beumer J, Clevers H. Establishment and Culture of Human Intestinal Organoids Derived from Adult Stem Cells. *Curr Protocols Immunol.* **2020**;130(1):e106. doi:10.1002/cpim.106
29. Mohammadi S, Morell-Perez C, Wright CW, et al. Assessing donor-to-donor variability in human intestinal organoid cultures. *Stem Cell Reports.* **2021**;16(9):2364–2378. doi:10.1016/j.stemcr.2021.07.016
30. Lin J, Huang L, Xiang R, et al. Blood compatibility evaluations of CaCO₃ particles. *Biomed Mater.* **2021**;16(5):055010. doi:10.1088/1748-605X/ac19bf
31. Mohamed AS, Fahmy SR, Soliman AM, Gaafar KM. Effects of 3 Rodent Beddings on Biochemical Measures in Rats and Mice. *J Am Assoc Lab Anim Sci.* **2018**;57(5):443–446. doi:10.30802/AALAS-JAALAS-18-000023
32. Chen Y, Qu D, Fu R, et al. A Tf-modified tripteryne-loaded coix seed oil microemulsion enhances anti-cervical cancer treatment. *Int J Nanomedicine.* **2018**;13:7275–7287. doi:10.2147/IJN.S182475
33. Cheng MB, Wang JC, Li YH, et al. Characterization of water-in-oil microemulsion for oral delivery of earthworm fibrinolytic enzyme. *J Controlled Release.* **2008**;129(1):41–48. doi:10.1016/j.jconrel.2008.03.018
34. Raskov H, Burcharth J, Pommergaard HC, Rosenberg J. Irritable bowel syndrome, the microbiota and the gut-brain axis. *Gut Microbes.* **2016**;7(5):365–383. doi:10.1080/19490976.2016.1218585
35. Ford AC, Sperber AD, Corsetti M, Camilleri M. Irritable bowel syndrome. *Lancet.* **2020**;396(10263):1675–1688. doi:10.1016/S0140-6736(20)31548-8
36. Li H, Wang T, Shi C, et al. Inhibition of GALR1 in PFC Alleviates Depressive-Like Behaviors in Postpartum Depression Rat Model by Upregulating CREB-BDNF and 5-HT Levels. *Front Psychiatry.* **2018**;9:588. doi:10.3389/fpsy.2018.00588
37. Rosa K, Delgado-Herrera L, Zeiher B, et al. Psychometric assessment of the IBS-D Daily Symptom Diary and Symptom Event Log. *Quality Res.* **2016**;25(12):3197–3208. doi:10.1007/s11136-016-1335-1